Search for a circum-planetary material and orbital period variations of short-period Kepler exoplanet candidates

Z. Garai[1,⋆], **G. Zhou**[3], **J. Budaj**[3,1], and **R.F. Stellingwerf**[2]

[1] Astronomical Institute, Slovak Academy of Sciences, 059 60 Tatranska Lomnica, Slovak Republic
[2] Stellingwerf Consulting, 11033 Mathis Mtn Rd SE, Huntsville, AL 35803, United States of America
[3] Research School of Astronomy and Astrophysics, Australian National University, Canberra, ACT 2611, Australia

Received dd mmm yyyy, accepted dd mmm yyyy
Published online dd mmm yyyy

Key words Stars: planetary systems – techniques: photometric

A unique short-period ($P = 0.65356(1)$ days) Mercury-size Kepler exoplanet candidate KIC012557548b has been discovered recently by *Rappaport et al. (2012)*. This object is a transiting disintegrating exoplanet with a circum-planetary material – comet-like tail. Close-in exoplanets, like KIC012557548b, are subjected to the greatest planet-star interactions. This interaction may have various forms. In certain cases it may cause formation of the comet-like tail. Strong interaction with the host star, and/or presence of an additional planet may lead to variations in the orbital period of the planet.
Our main aim is to search for comet-like tails similar to KIC012557548b and for long-term orbital period variations. We are curious about frequency of comet-like tail formation among short-period Kepler exoplanet candidates. We concentrate on a sample of 20 close-in candidates with a period similar to KIC012557548b from the Kepler mission.
We first improved the preliminary orbital periods and obtained the transit light curves. Subsequently we searched for the signatures of a circum-planetary material in these light curves. For this purpose the final transit light curve of each planet was fitted with a theoretical light curve, and the residuals were examined for abnormalities. We then searched for possible long-term changes of the orbital periods using the method of phase dispersion minimization.
In 8 cases out of 20 we found some interesting peculiarities, but none of the exoplanet candidates showed signs of a comet-like tail. It seems that the frequency of comet-like tail formation among short-period Kepler exoplanet candidates is very low. We searched for comet-like tails based on the period criterion. Based on our results we can conclude that the short-period criterion is not enough to cause comet-like tail formation. This result is in agreement with the theory of the thermal wind and planet evaporation (Perez-Becker & Chiang 2013). We also found 3 cases of candidates which showed some changes of the orbital period. Based on our results we can see that orbital period changes are not caused by comet-like tail disintegration processes, but rather by possible massive outer companions.

© 2006 WILEY-VCH Verlag GmbH & Co. KGaA, Weinheim

arXiv:1410.1290v1 [astro-ph.EP] 6 Oct 2014

1 Introduction

Close-in exoplanets are subjected to the greatest planet-star interactions. It may have various forms. (1) Heavy irradiation changes the atmospheric structure and creates a deep temperature plateau or a stratosphere (Hubeny, Burrows & Sudarsky 2003; Burrows, Budaj & Hubeny 2008; Knutson et al. 2008; Fortney et al. 2008). (2) Strong irradiation drives the mass loss from the planet (Burrows & Lunine 1995; Guillot et al. 1996). It was detected in HD 209458b (Vidal-Madjar et al. 2003, 2004), and in HD 189733b (Lecavelier des Etangs et al. 2010; Bourrier et al. 2013). Several theoretical studies were devoted to this subject (e.g. Yelle 2004; Tian et al. 2005; Hubbard et al. 2007; Lopez, Fortney & Miller 2012). *Kurokawa & Kaltenegger (2013)* developed a combined model of atmospheric mass loss calculation and thermal evolution calculation of a planet. *Owen & Wu (2013)* concluded that evaporation is the driving force of evolution for close-in Kepler exoplanets. It is therefore plausible to assume that some close-in exoplanets may be surrounded by a circum-planetary material. (3) Strong interaction with the host star forces the planet into synchronization and circularization of its rotation and orbit (Zahn 1977; Tassoul & Tassoul 1992; Bodenheimer, Lin & Mardling 2001). (4) Strong interaction with the host star, and/or presence of an additional planet may lead to variations in the orbital period of the planet (Agol et al. 2005; Holman & Murray 2005; Ford et al. 2011, 2012; Steffen et al. 2012; Maciejewski et al. 2013; Mazeh et al. 2013).

Kepler mission discovered thousands of new transiting extrasolar planet candidates (Borucki et al. 2011). The unprecedented photometric precission of Kepler has made it possible to detect transits by Earth size planets (Fressin et al. 2012; Borucki et al. 2012), planetary optical secondary eclipses and phase variations (see e.g. Jackson et al. 2014; Sanchis-Ojeda et al. 2014; Esteves, De Mooij & Jayawardhana 2013 and references therein), amongst other subtle phenomena.

A unique close-in Mercury-size Kepler exoplanet candidate KIC012557548b has been discovered recently by

⋆ Corresponding author: e-mail: zgarai@ta3.sk

© 2006 WILEY-VCH Verlag GmbH & Co. KGaA, Weinheim

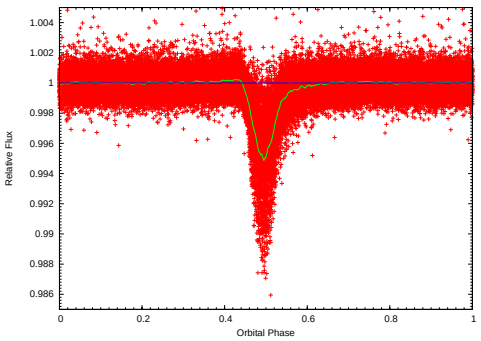

Fig. 1 The transit light curve of KIC012557548b with the transit (Borucki et al. 2011; analyzed by Budaj 2013). It is best represented by an exoplanet with a comet-like tail.

Rappaport et al. (2012). Unlike all other exoplanets it exhibits significant variability in the transit depth (Fig. 1). The shape of the transit is highly asymmetric, with a significant brightening just before the eclipse, sharp ingress followed by a smooth egress (Fig. 2). The light curve of this planet was studied in more detail by *Brogi et al. (2012)*, *Budaj (2013)*, *Kawahara et al. (2013)*, *Croll et al. (2014)*, and *van Werkhoven et al. (2014)*. The planet also has an extremely short orbital period of 0.65356(1) days (15.6854 hours). The host star that is apparently being occulted is KIC012557548, a V = 16 magnitude K-dwarf with $T_{eff} \simeq 4400$ K. *Rappaport et al. (2012)* suggested that the planet has size not larger than Mercury, and is slowly disintegrating/evaporating, creating a comet-like tail. *Perez-Becker & Chiang (2013)* proposed a model of the atmosheric escape via the thermal wind. It is effective only for planets which are less massive than Mercury. Gravity of the more massive planets would provide too deep potential barier for the wind. Another close-in Kepler exoplanet candidate KIC8639908b ($R_p \leq 1.06 R_\oplus$), detected recently also by *Rappaport et al. (2014)* with an orbital period of 0.910022(5) days, exhibits a distinctly asymmetric transit profile, likely indicative of the emission of dusty effluents, and reminiscent of KIC012557548b. The host star has $T_{eff} \simeq 4435$ K, it is a V = 15.9 magnitude K-dwarf. Mass loss and possible comet-like tail was detected also in GJ 436b in Lyα by *Kulow et al. (2014)*.

In this paper, we search for evidence of disintegration in the shortest period Kepler exoplanet candidates, by examining their transit light curves for asymmetric features. The layout of the paper is as follows. In *Section 2*, we provide an overview of our exoplanet sample. In *Section 3*, we describe the data analysis and in *Section 4* our motivation. *Section 5* is the main part of our work. It describes obtained results. Our findings are summarized in *Section 6*.

2 Motivation, aims and sample selection

Our main aim is to search for comet-like tails similar to KIC012557548b and for long-term orbital period variations. We are curious about frequency of comet-like tail formation among short-period Kepler exoplanet candidates. Close-in exoplanets, like KIC012557548b, are subjected to the greatest planet-star interactions. We therefore concentrate on the short-period exoplanet candidates with periods similar to KIC012557548b. Kepler mission exoplanet candidates are described in the catalog of *Batalha et al. (2013)*. From this catalog we chose a sample of 20 candidates with the shortest orbital period. An overview of our sample is in *Table 1*. This sample covers the orbital periods in the range of 0.370 to 0.708 days, and stellar effective temperatures in the range of $T_{eff} \simeq 3900 - 6600$ K. Consequently, the incident flux hitting the exoplanet may not be exactly the same as in the case of KIC012557548b, but may slightly vary by about 1-2 orders of magnitude.

Table 1 An overview of our sample (Batalha et al. 2013). This sample covers the orbital periods in the range of 0.370 to 0.708 days, and stellar effective temperatures in the range of $T_{eff} \simeq 3900 - 6600$ K.

KIC Number	Orbital period (days)	T_{eff} (K)
3848972	0.3705290	5286
8561063	0.4532875	4188
6666233	0.5124040	3932
6047498	0.5187486	5359
9030447	0.5667281	6693
6934291	0.5678562	4927
4055304	0.5710391	5022
10024051	0.5773752	5062
8235924	0.5879933	4003
11774303	0.6140747	6271
10975146	0.6313298	4369
10028535	0.6630983	4994
10468885	0.6640818	5013
11600889	0.6693163	5627
8278371	0.6773911	5731
5513012	0.6793614	5375
10319385	0.6892040	5719
9761199	0.6920069	4060
9473078	0.6938521	5353
5972334	0.7085982	5495

3 Light curve analysis and model fitting

We used the publicly available 17 quarter Kepler data in the form of Pre-search Data Conditioning Simple Aperture Photometry (PDCSAP) fluxes. Only the long cadence data were used, as they are sufficient in revealing the large-scale asymmetries caused by circum-planetary material. Kepler observations were treated and analysed similarly as in *Budaj (2013)*. There is an offset between Kepler fluxes from different quarters. Consequently, fluxes within each quarter were normalized to unity. We then improved the preliminary orbital period of the exoplanet (Batalha et al. 2013)

© 2006 WILEY-VCH Verlag GmbH & Co. KGaA, Weinheim

using the method of phase dispersion minimization (PDM) described later. The data were cut into segments each covering one orbital period. Each segment of data was fitted with a linear function. During the fitting procedure the part of the data covering the transit was excluded from the fit. Consequently, the linear trend was removed from each chunk of data (including the transit data). The final value of the orbital period was then found in this detrended data. Finally the data were phased with this new orbital period. We used phase 0.5 for transits. This method can effectively remove the long term variability (mainly variability of the host star due to spots and rotation) while it does not introduce any nonlinear trend to the phase light curve. To reduce the noise, the phased light curve was subject to a running window averaging. We used a window with the width of 0.01 and step of 0.001 (in units of phase) in all cases.

We searched for the signatures of a circum-planetary material in these light curves. For this purpose the final transit light curve of each planet was fitted with a theoretical light curve (see left panels in appendix A), and the residuals were examined for abnormalities (see mid panels in appendix A). We employed the *Mandel & Agol (2002)* transit model with the free parameters: mid transit time T_c (in TDB-based BKJD), period P (days), planet-to-star radius ratio R_p/R_s, normalised semi-major axis $(R_p+R_s)/a$, line-of-sight inclination i (deg), and quadratic limb darkening parameters $q_1 = (u_1+u_2)^2$ and $q_2 = 0.5u_1(u_1+u_2)^{-1}$ parameterised as per *Kipping (2013)*. We first compute the light curve for a single transit epoch, sampled at 0.0005 in phase (< 1 minute sampling for a 1 day period candidate). The model light curve is then convolved with a box-car with width of 30 minutes, simulating the integration time of a long-cadence exposure. This template transit model is then interpolated using a B-spline, and evaluated at the time stamps of the observed light curve to arrive at the final model. To speed up the computation process, we reduce the number of points by selecting only the in-transit and 0.1 phase of the out-of-transit portions of the light curve for the fitting. This cropping of the light curve is justified since we are interested in only the distortions to the transit shape, not the out-of-transit variations. To find the best fit parameters and explore the degeneracies and uncertainties, we perform a Markov Chain Monte Carlo (MCMC) minimisation using the *emcee* ensemble sampler (Foreman-Mackey et al. 2013). To better account for sources of errors in the photometry, individual measurement errors of the light curves are inflated such that the reduced χ^2 is at unity before the MCMC routine, enabling a more realistic estimate the posterior probability distribution. The best fit parameters and their errors are derived from the marginalised posterior probability distributions after the MCMC analysis.

We also searched for possible long-term changes of the orbital period. First we improved the preliminary orbital period of the extrasolar planet using the method of phase dispersion minimization (PDM – Stellingwerf 1978; application PDM2 ver. 4.13[1] – Stellingwerf 2004) and then using the Fourier analysis (FA). The detrended data were used for this purpose (as described earlier in this section). We assumed that the period changes linearly:

$$P = P_0 + \beta t \quad (1)$$

where β is a dimensionless value, but is often expressed in days/million years (d/Myr). The output from the analysis (PDM2 4.13 in this case) is a curve (see right panels in appendix A), which shows the dependence of Θ_{min} as a function of β. Θ_{min} is a dimensionless statistical parameter (Stellingwerf 1978). The minimum value of Θ_{min} indicates the value of the period change – β.

For candidates where the PDM analysis indicated potential period variations, we broke the light curve into segments of 2000/4000 points, and re-performed the MCMC analysis. The minimisation is performed globally such that all the light curve segments are fitted simultaneously, allowing individual T_c values for each segment of the light curve, but shared transit geometry parameters R_p/R_s, $(R_p + R_s)/a$, and i. We fixed P to the best fit period from the initial analysis. The fitted T_c values are then inspected for non-linear variations with respect to the centre time of each light curve segment.

4 Exoplanet candidate KIC012557548b

To test the effectiveness of our techniques, we first applied the procedure, described above, to this exoplanet candidate.

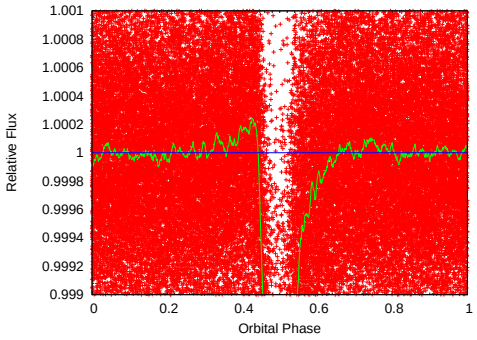

Fig. 2 The transit light curve of KIC012557548b (Borucki et al. 2011; analyzed by Budaj 2013), cropped to enhance the asymmetric features. It shows a significant pre-transit brightening, sharp ingress followed by a short sharp egress and long smooth egress, and a weak post-transit brightening.

KIC012557548b can be used as an extreme example of the exoplanet with a circum-planetary material. It was discovered by *Rappaport et al. (2012)*. The light curve of the Kepler exoplanet candidate KIC012557548b is peculiar and

[1] Actual version of the software package is available on the webpage http://www.stellingwerf.com

© 2006 WILEY-VCH Verlag GmbH & Co. KGaA, Weinheim

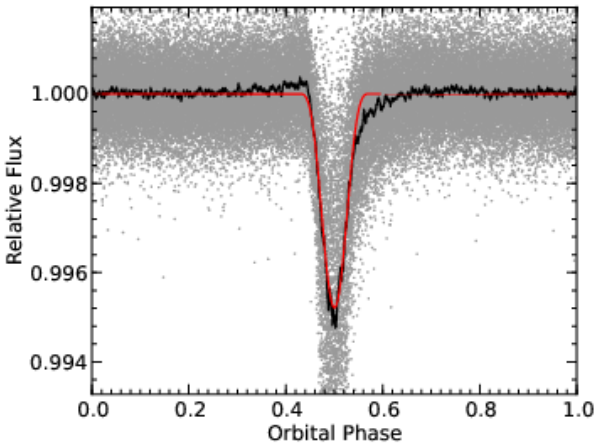

Fig. 3 The transit light curve of KIC012557548b with the transit (Borucki et al. 2011; analyzed by Budaj 2013). It was fitted with a theoretical light curve similarly as light curves in *appendix A* (see Section 3 and left panels in appendix A).

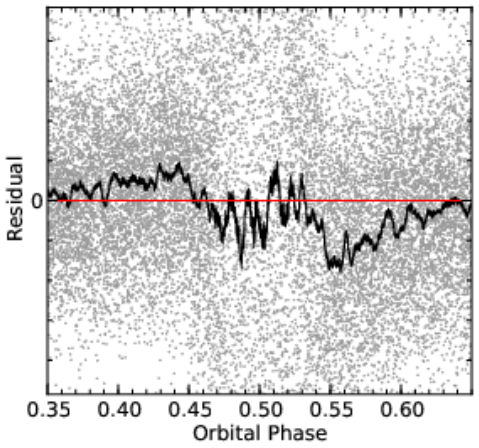

Fig. 4 The transit residuals of KIC012557548b obtained similarly as transit residuals in *appendix A* (see Section 3 and mid panels in appendix A). A standard Mandel-Agol transit fits this candidate poorly. We can see the pre-transit brightening between $0.39 < P < 0.45$, as well as the smooth egress between $0.55 < P < 0.65$. Large scatter observed between $0.45 < P < 0.55$ indicate the variability in the transit depth.

very interesting. It shows a significant brightening just before the eclipse – pre-transit brightening, sharp ingress followed by a short sharp egress and long smooth egress, and a weak post-transit brightening (Brogi et al. 2012; Budaj 2013). A close-up of the transit features are shown in *Fig. 2*.

Moreover, the candidate exhibits strong variability in the transit core on timescale of one day (Rappaport et al. 2012), and variability in the egress on the timescale of about 1.3 years (Budaj 2013). *Rappaport et al. (2012)* suggest that KIC012557548b is a slowly disintegrating/evaporating planet what creates a comet-like tail. *Brogi et al. (2012)* and *Budaj (2013)* reanalyzed the light curve in detail and both validated the disintegrating-planet scenario by modeling. Both brightenings are caused by the forward scattering on dust particles in the tail, which have typical radii of about 0.1-1 micron. Strong variability in the transit depth is a consequence of changes in the cloud optical depth.

Subsequently, we fitted the observed light curve with the theoretical model light curve, assuming a spherical planet (Fig. 3), and obtained transit residuals of KIC012557548b (Fig. 4) as per *Section 3*. The best fit quadratic limb darkening coefficients were $q_1 = 0.98(8)$ and $q_2 = 0.98(7)$. The best fit system parameters are: mid transit time $T_c = 0.0404(2)$ (BKJD), period $P = 0.65355$ days, planet-to-star radius ratio $R_p/R_s = 0.3(1)$, normalised semi-major axis $(R_p + R_s)/a = 0.60(5)$, and line-of-sight inclination $i = 58(4)$ (deg). *Fig. 4* shows a significant fluctuation in these residuals. This signature of the residuals indicate the circum-planetary material. The residuals also reveal the pre-transit brightening between $0.39 < P < 0.45$, as well as the smooth egress between $0.55 < P < 0.65$. We can see the pre-transit brightening as a positive fluctuation, and the smooth egress as a negative fluctuation. Large scatter observed between $0.45 < P < 0.55$ indicate the variability in the transit depth. These additional features of transit residuals suggest the comet-like tail.

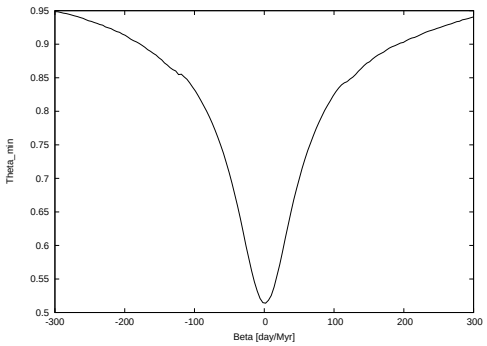

Fig. 5 Serach for a long-term change of the orbital period of KIC012557548b based on 17 quarter data. Figure shows that there is no significant evidence for the long-term period change.

We then searched for evidence of transit-timing variations in KIC012557548b using the PDM method. Since KIC012557548b is close-in exoplanet candidate that is apparently being disintegrated and losing material, one might expect all kinds of interaction that could lead to the long-term period variation. That is why *Budaj (2013)* also searched for possible long-term changes of the orbital period with the PDM method (Stellingwerf 1978; application PDM2 4.13 – Stellingwerf 2004). He obtained $\beta = 0.3 \pm 0.5$ d/Myr, which means that there is no significant evidence for the long-term period change. Since *Budaj (2013)* searched

© 2006 WILEY-VCH Verlag GmbH & Co. KGaA, Weinheim

for possible long-term changes of the orbital period based on 14 quarters of Kepler data, we repeated this analysis using 17 quarters of data. We can confirm the author's result that there is no significant evidence for the long-term orbital period variation: $\beta = 0.9 \pm 1.1$ d/Myr (Fig. 5). We also improved the orbital period of the exoplanet KIC012557548b and obtained $P = 0.65355390$ days using the PDM and $P = 0.65355380$ days using the FA method. These results are very similar to the fit period result. These values are also in the good agreement with the values reported in *Rappaport et al. (2012)*, *Budaj (2013)*, and *van Werkhoven et al. (2014).*

5 Results

The following subsections include a description of the candidates, formated as per our discussion of KIC012557548b. Each subsection includes results from both (1) analysis of the transit residuals, where we searched for comet-like tails similar to KIC012557548b, and (2) analysis of the orbital periods, where we searched for long-term orbital period variations. Interesting exoplanet candidates are described in individual subsections. The last subsection includes the exoplanets that do not show any significant features.

5.1 Exoplanet candidate KIC3848972

The Kepler exoplanet candidate KIC3848972 is interesting for several reasons. Although the transit light curve (Fig. A1 – see left panel) does not show signs of a pre-transit brightening, post-transit brightening, nor significant variability in the transit depth, an other hand its transit is significantly deeper (0.002) then transits of other planets from our sample, and it has a V-type shape, which might indicate a grazing eclipsing binary. Subsequently, we fitted the light curve (Fig. A1 – see left panel) and obtained transit residuals of KIC3848972 (Fig. A1 – see mid panel). The transit residuals of KIC3848972 show only a linear downward trend from sine-like background variability. We obtained the best fit quadratic limb darkening coefficients of $q_1 = 0.9(1)$ and $q_2 = 0.9(3)$ for the star. The best fit system parameters are: mid transit time $T_c = 534.34045(5)$ (BKJD), period $P = 0.37053$ days, planet-to-star radius ratio $R_p/R_s = 0.18(8)$, normalised semi-major axis $(R_p + R_s)/a = 0.71(4)$, and line-of-sight inclination $i = 49(6)$ (deg). The parameter $R_p/R_s = 0.0435$, presented by *Batalha et al. 2013*, is very different from what we got for R_p/R_s, due to the degeneracy between R_p/R_s, inclination i, and $(R_p+R_s)/a$. Indeed *Colón, Ford & Morehead (2012)*, based on a significant color change during the transit event, identify KIC3848972 as a false positive, which may consist of an evolved giant star that is redder and several magnitudes brighter than the eclipsing star. *Slawson et al. (2011)* found an orbital period for this system that is twice as long. Moreower, we found a small difference between the odd and even transits in this system (0.000140) and a weak periodic background variability, which is very similar to an RS Canum Venaticorum-like distortion wave (see e.g. Luddington 1978). That is why we consider the eclipsing binary alternative as possible. We also observed a similar peculiarity at KIC9761199 (see subsection 5.7). On *Fig. 6* we can see that the sine-like distortion wave is extends throughout the double-period phase folded light curve. The distortion wave is slightly shifting in phase during the Kepler observations, but we always observed only one sine-wave. The background variations may potentially be due to spot modulation from one of the stars.

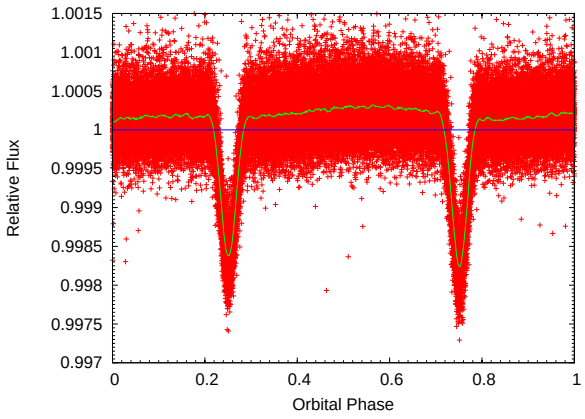

Fig. 6 The double-period phase-folded light curve of KIC3848972. The system exhibits a small difference between the odd and even transits, and a sinusoidal background variability.

Next we searched for long-term orbital period changes. First we improved the orbital period. We obtained period $P = 0.37052870$ days using the PDM and $P = 0.37052750$ days using the FA method, which are very similar to the fit period result. These values are also in the good agreement with the value $P = 0.3705290$ days, reported in *Batalha et al. (2013)*. However, based on our period analysis, the two times alias orbital period is also possible. If the period is indeed two times longer, both stars would have very similar temperatures. *Fig. A1 – right panel* shows that there is no significant evidence for the long-term period change ($\beta = -0.8 \pm 1.4$ d/Myr).

5.2 Exoplanet candidate KIC8561063

The Kepler exoplanet candidate KIC8561063 is similar to the previous exoplanet candicate. It shows relatively deep transit (0.0015) with a V-type shape, which needs to be checked, since it may be indicative of an eclipsing binary (Fig. A2 – see left panel). An other hand, we do not find significant difference between the odd and even transits in this system. The light curve also does not show any signs of a pre-transit brightening, post-transit brightening, nor significant variability in the transit depth. We modelled the transit light curve and obtained transit residuals from 0.35 to 0.65

© 2006 WILEY-VCH Verlag GmbH & Co. KGaA, Weinheim

in phase units. They are depicted in *Fig. A2 – mid panel*, and also do not show any signs of a comet-like tail. The fitting derived model has quadratic limb darkening coefficients of $q_1 = 0.0001(8)$ and $q_2 = 0.7(1)$. The best fit system parameters are: mid transit time $T_c = 488.7930(1)$ (BKJD), period $P = 0.45329$ days, planet-to-star radius ratio $R_p/R_s = 0.044(4)$, normalised semi-major axis $(R_p + R_s)/a = 0.2(1)$, and line-of-sight inclination $i = 76(2)$ (deg).

Subsequently, we improved the orbital period and obtained $P = 0.45328705$ days using the PDM and $P = 0.45328830$ days using the FA method, which are very similar to the fit period result. However, based on our period analysis, the two times alias orbital period is also possible. If the period is indeed two times longer, both stars would have the same temperatures. *Fig. A2 – right panel* shows that there is no significant evidence for the long-term period evolution ($\beta = 0.92 \pm 0.93$ d/Myr).

5.3 Exoplanet candidate KIC6666233

Its transit (Fig. A3 – left panel) is shallower (0.00037) then transits mentioned above, and has an U-shape, which is typical for exoplanet transits. At the same, we detected a small difference between the odd and even transits (0.000054; see Fig. 7), potentially indicative of an eclipsing binary system with twice the orbital period.

Subsequently, we modelled the transit light curve (Fig. A3 – see left panel). The best fit limb darkening coefficients of the star were $q_1 = 0.26(4)$ and $q_2 = 0.8(1)$. The best fit system parameters are: mid transit time $T_c = 546.2643(5)$ (BKJD), period $P = 0.51241$ days, planet-to-star radius ratio $R_p/R_s = 0.016(2)$, normalised semi-major axis $(R_p + R_s)/a = 0.27(1)$, and line-of-sight inclination $i = 85(4)$ (deg). The light curve and transit residuals (Fig. A3 – left and mid panels) do not show any indication of the circum-planetary material.

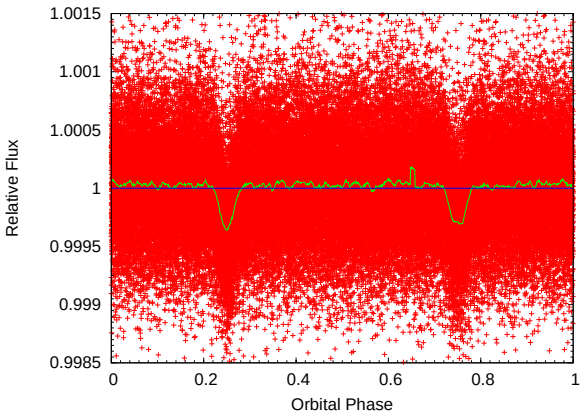

Fig. 7 The double-period phase-folded light curve of KIC6666233 with a small depth difference between the odd and even transits in this system.

We improved the orbital period and obtained $P = 0.51240883$ days using the PDM and $P = 0.51240860$ days using the FA method. These values are in the good agreement with the value $P = 0.5124040$ days, reported in *Batalha et al. (2013)*. However, based on our period analysis, the two times alias orbital period is still possible. There is no significant evidence for the long-term period change ($\beta = -1.0 \pm 2.3$ d/Myr).

5.4 Exoplanet candidate KIC6047498

The light curve of this candidate (Fig. A4 – left panel) exhibits a V-shaped transit with depth of 0.0007, showing no pre-transit brightening, post-transit brightening, nor significant variability in the transit depth. The transit residuals also do not show any signs of a comet-like tail (Fig. A4 – see mid panel). The best fit quadratic limb darkening coefficients were $q_1 = 0.94(5)$ and $q_2 = 0.95(4)$. The best fit system parameters are: mid transit time $T_c = 534.1331(3)$ (BKJD), period $P = 0.51873$ days, planet-to-star radius ratio $R_p/R_s = 0.3(2)$, normalised semi-major axis $(R_p + R_s)/a = 0.76(5)$, and line-of-sight inclination $i = 43(5)$ (deg). The parameter $R_p/R_s = 0.02919$, presented by *Batalha et al. (2013)*, is very different from our derived R_p/R_s, due to the degeneracy between R_p/R_s, inclination i, and $(R_p + R_s)/a$. We also detected a small difference between the odd and even transits in this system (0.000135; see Fig. 8), which is similar to the difference measured at the candidate KIC3848972.

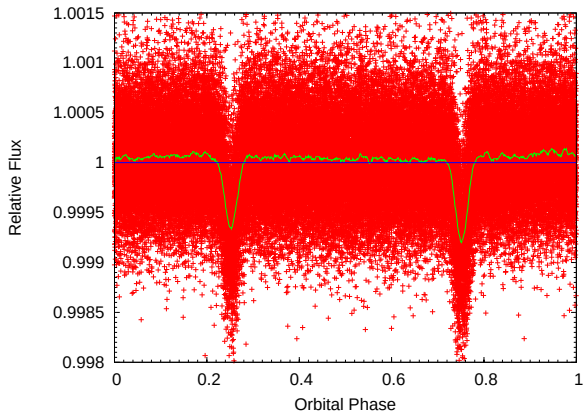

Fig. 8 The double-period phase-folded light curve of KIC6047498 with a small difference between the odd and even transits in this system.

Further we searched also for a long-term orbital period change. First we improved the orbital period. We obtained period $P = 0.51872845$ days using the PDM and $P = 0.51872930$ days using the FA method, which are in the good agreement with the fit period result, and also with the value presented by *Batalha et al. (2013)*, with the possibility of the two times alias. *Fig. A4 – right panel* shows that there is possible evidence for the long-term period change,

© 2006 WILEY-VCH Verlag GmbH & Co. KGaA, Weinheim

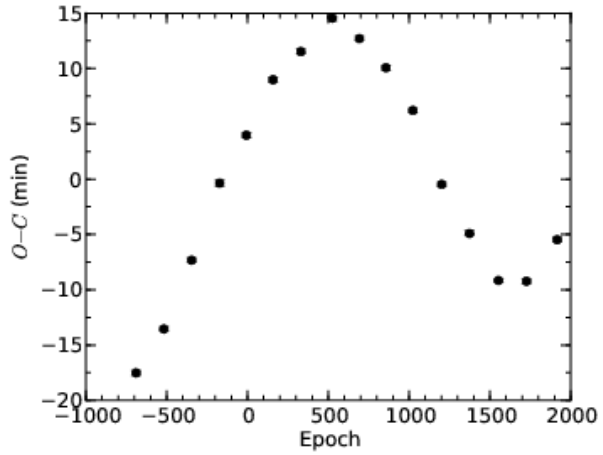

Fig. 9 The T_c-free MCMC analysis in case of KIC6047498. Figure shows the O-C diagram of mid transit time variations. The O-C exhibits a semi-periodic TTV variability, indicative of an outer companion with an orbital period of $>$ 2000 days.

$\beta = -15.05017 \pm 1.94760$ d/Myr, that means a potential shortening of the orbital period. Since the PDM analysis indicated a potential period variation, we broke the light curve into segments of 4000 points in this case, and re-performed the T_c-free MCMC analysis. This analysis confirmed our results from the PDM analysis about long-term period change. We found a semi-periodic TTV signal associated with the transit, indicative of an outer companion with an orbital period of $>$ 2000 days (Figs. 9 and 10).

5.5 Exoplanet candidate KIC9030447

The light curve of the exoplanet candidate KIC9030447 is peculiar (Fig. A5 – see left panel). It shows a small brightening, approximately half a phase from the transit, and a secondary eclipse-like signal approximately at phase 0.85. Subsequently, we obtained the model light curve and transit residuals of the exoplanet candidate. The best model fit did not describe the transit well. The best fit quadratic limb darkening coefficients of the star were $q_1 = 0.47(2)$ and $q_2 = 0.99(2)$. The best fit system parameters are: mid transit time $T_c = 534.478(1)$ (BKJD), period $P = 0.56677$ days, planet-to-star radius ratio $R_p/R_s = 0.0091(1)$, normalised semi-major axis $(R_p + R_s)/a = 1.000(8)$, and line-of-sight inclination $i = 85(1)$ (deg). The transit residuals of this exoplanet candidate reflect the peculiarities of the light curve, and residual fluctuations due to the poor fit (see Fig. A5 – mid panel). *Ofir & Dreizler (2013)* proposed that such behavior is caused by pulsations, rather than transits or eclipses. Further we discovered that these additional features of the light curve slighly shifted in phase during the Kepler observations. Moreover, the secondary eclipse-like signal is changing its depth. That is why we consider the eclipsing binary on eccentric orbit alternative as more possible.

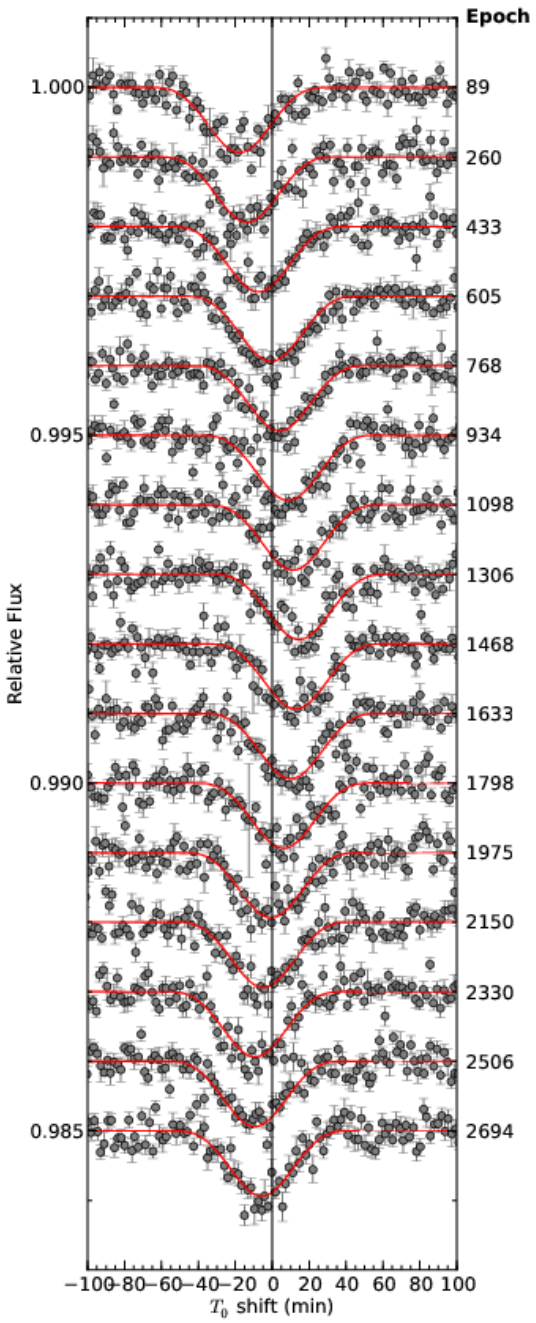

Fig. 10 The transit for each segment of the KIC6047498 light curve, with best fit model overplotted. The mean transit epochs for each segment are labelled on the left. Each segment is arbitrarily shifted vertically for clarity. The solid vertical line shows the mean T_c value. The transit centres are visibly shifted from segment to segment.

Subsequently, we improved the orbital period and obtained $P = 0.56670873$ days using the PDM and $P = 0.56680630$ days using the FA method. *Fig. A5 – right panel*

© 2006 WILEY-VCH Verlag GmbH & Co. KGaA, Weinheim

shows that there is no significant evidence for the long-term period change ($\beta = 0.9 \pm 8.6$ d/Myr).

5.6 Exoplanet candidate KIC11774303

On first glance, the light curve of this exoplanet candidate does not show any significant peculiarity. The transit residuals also do not show any convincing systematic fluctuations, and indicate that the light curve can be described well by the standard transit model (Fig. A10 – left and mid panels). The best fit quadratic limb darkening coefficients of the star were $q_1 = 0.118(9)$ and $q_2 = 0.7(2)$. The best fit system parameters are: mid transit time $T_c = 457.3181(7)$ (BKJD), period $P = 0.61408$ days, planet-to-star radius ratio $R_p/R_s = 0.07(4)$, normalised semi-major axis $(R_p + R_s)/a = 0.8(1)$, and line-of-sight inclination $i = 37(11)$ (deg). However, *Ofir & Dreizler (2013)* detected significant differences between the odd and even transits in this system, and suggested that this candidate is an eclipsing binary with twice the period. We also measured a transit depth difference (0.000228; Fig. 11) and we could confirm their conclusions about transit differences. Based on this result we consider the eclipsing binary alternative as possible.

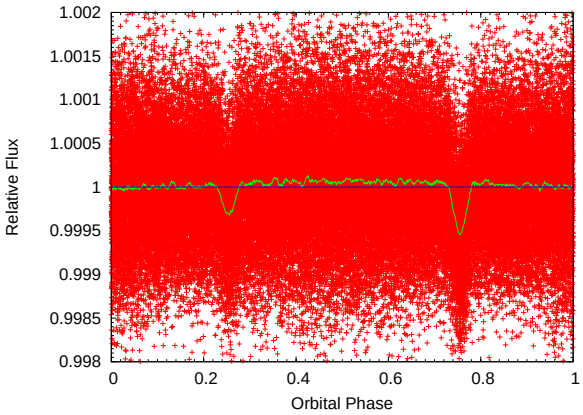

Fig. 11 The double-period phase-folded light curve of KIC11774303 with a difference in depth between the odd and even transits in this system.

An other hand, we improved the orbital period and obtained period $P = 0.61408403$ days using the PDM and $P = 0.61409220$ days using the FA method, in agreement to the fit period result, but we could not confirm the two times period alias using the PDM/FA analysis. *Fig. A10 – right panel* shows that there is no significant evidence for the long-term period change ($\beta = 0.9 \pm 2.9$ d/Myr).

5.7 Exoplanet candidate KIC9761199

The Kepler exoplanet candidate KIC9761199 is also very interesting. Its transit (Fig. A18 – see left panel) is very deep (0.0045) and has a V-type shape, which might indicate a grazing eclipsing binary. The transit light curve does not show any signs of a pre-transit brightening, post-transit brightening, nor significant variability in the transit depth. Apart from that, the out-of-transit light curve exhibits a periodic background variability, which is very similar to an RS Canum Venaticorum-like distortion wave (see e.g. Ludddington 1978). That is why we consider the eclipsing binary alternative as possible. The background variability is also very similar to the distortion wave observed by KIC3848972 (see subsection 5.1), but contrary to the KIC3848972, this wave is stronger. Subsequently, we fitted the light curve with a model light curve (Fig. A18 – see left panel) and obtained transit residuals of this exoplanet candidate from 0.35 to 0.65 in phase units (Fig. A18 – mid panel). The best fit quadratic limb darkening coefficients were $q_1 = 0.94(5)$ and $q_2 = 0.96(1)$. The best fit system parameters are: mid transit time $T_c = 533.1669(1)$ (BKJD), period $P = 0.69202$ days, planet-to-star radius ratio $R_p/R_s = 0.22(9)$, normalised semi-major axis $(R_p + R_s)/a = 0.43(3)$, and line-of-sight inclination $i = 68(2)$ (deg). The parameter $R_p/R_s = 0.06943$, presented by *Batalha et al. (2013)*, is very different from what we got for R_p/R_s, due to the degeneracy between R_p/R_s, inclination i, and $(R_p + R_s)/a$. The transit residuals show only a relatively stronger linear trend from sine-like background variability. Contrary to the KIC3848972, the linear trend in this case has an upward direction. *Ofir & Dreizler (2013)* proposed that KIC9761199 is an eclipsing binary with twice the orbital period as suggested by *Batalha et al. (2013)*. There is indeed a small difference of 0.000704 between the odd and even transits (see Fig. 12). On *Fig. 12* we can see that the sine-like distortion wave is extends throughout the double-period phase folded light curve. Subsequently, we discovered that the sine-wave slightly shifted in phase during the Kepler observation. Sometimes we could observe double sine-wave and sometimes single sine-wave throughout the double-period phase folded light curve.

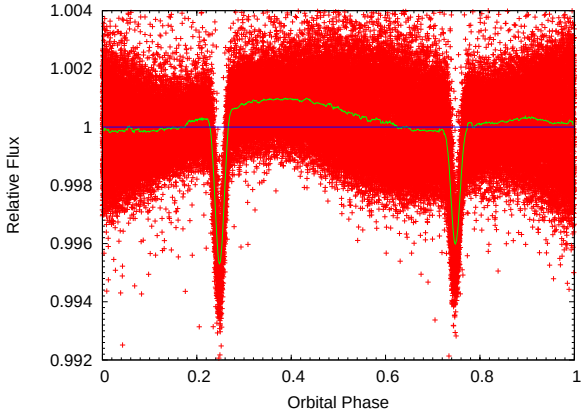

Fig. 12 The double-period phase-folded light curve of KIC9761199 with a small difference between the odd and even transits in this system and with a sinusoidal background variability.

© 2006 WILEY-VCH Verlag GmbH & Co. KGaA, Weinheim

The background variability may potentially be due to the Doppler beaming effect, sometimes also called Doppler boosting, induced by the stellar radial motion. This effect causes an increase (decrease) in the brightness of any light source approaching (receding from) the observer (e.g. Rybicki & Lightman 1979; Loeb & Gaudi 2003; Faigler & Mazeh 2011). We did not see any evidence of ellipsoidal and reflection phase variations from this system. In addition, the sinusoidal variability shifted in phase during the Kepler observations, suggesting that it is not due to beaming. The background variations may potentially be due to stellar spot modulation from both of the stars when we observe double sine-wave, and from one of the stars, when we observe single sine-wave throughout the double-period phase folded light curve.

Further we searched also for long-term orbital period change. First we improved the orbital period. We obtained period $P = 0.69201741$ days using the PDM and $P = 0.69204530$ days using the FA method. These values are in the good agreement with the value $P = 0.69202$ days obtained by the fitting procedure, and also in the good agreement with the value $P = 0.6920069$ days reported by *Batalha et al. (2013)*, but based on our period analysis, the two times period alias could not be ruled out. *Fig. A18 – right panel* shows that there is a possible evidence for the long-term period change, with $\beta = -3.01003 \pm 0.43245$ d/Myr, which means a potential shortening of the orbital period. Since the PDM analysis indicates a potential period variation, we broke the light curve into segments of 2000 points in this case, and re-performed the T_c-free MCMC analysis. This analysis confirmed our results from the PDM analysis about long-term period change, and revealed a periodic TTV signal with a period of ~ 1500 days, indicative of a possible massive outer companion (Figs. 13 and 14).

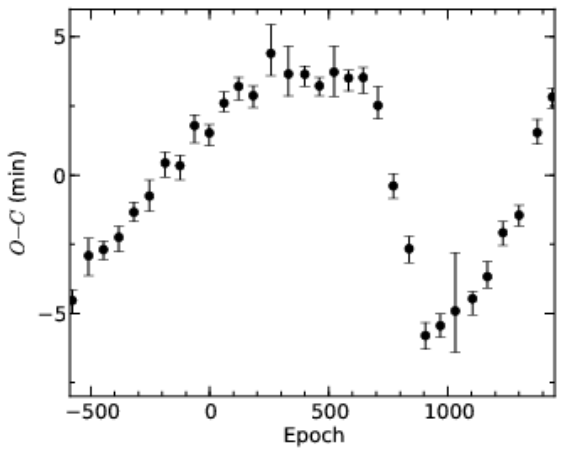

Fig. 13 The T_c-free MCMC analysis in case of KIC9761199. Figure shows the O-C diagram of mid transit time variations. We found a periodic TTV signal with a period of ~ 1500 days, indicative of a possible massive outer companion.

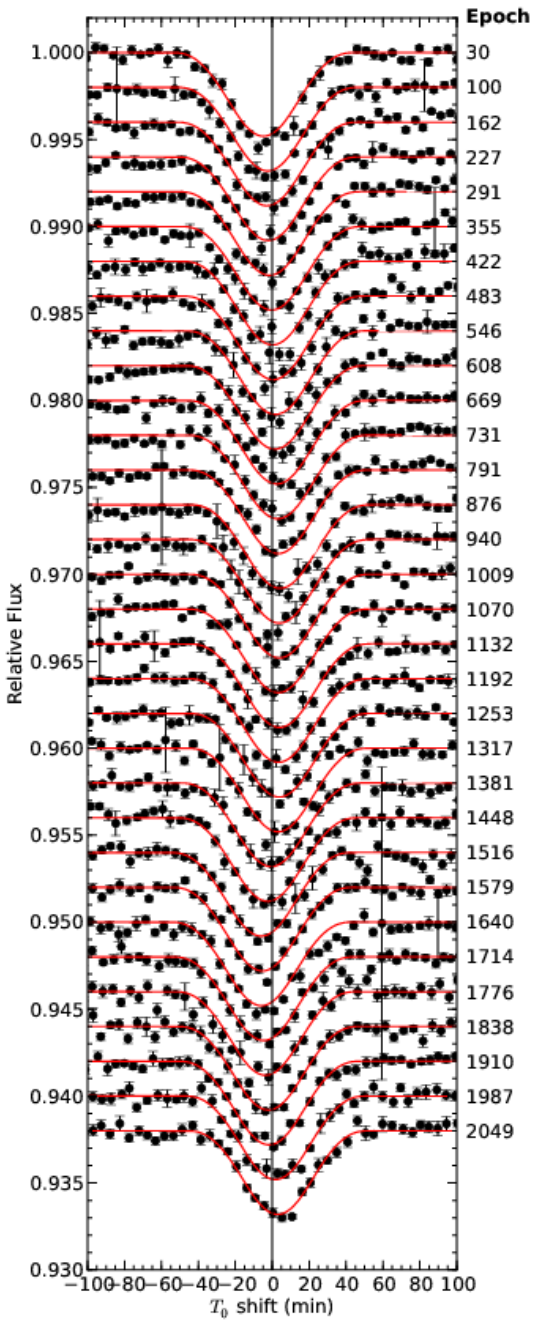

Fig. 14 The transit for each segment of the KIC9761199 light curve, with best fit model overplotted. For details see *Fig. 10*.

5.8 Exoplanet candidate KIC5972334

The Kepler exoplanet candidate KIC5972334 is another interesting object in our sample. We first obtained the light curve using the period $P = 0.7085982$ days reported by *Batalha et al. (2013)*. It is shown in *Fig. 15*. We did not find a convincing transit signal at this orbital period. We searched for periods and obtained $P = 15.35747382$ days

© 2006 WILEY-VCH Verlag GmbH & Co. KGaA, Weinheim

using the PDM and $P = 15.36051120$ days using the FA method. We did not confirm the preliminary orbital period. According to these results the light curve of KIC5972334 was reanalysed with $P = 15.35747382$ days. *Steffen et al. (2010)* suggested that this star shows transits from two exoplanets with orbital period $P = 15.359$ days and $P = 2.420$ days. We confirmed the first period, but could not confirm the second object via PDM/FA period analysis. The transit light curve folded with the period $P = 15.35747382$ days is shown in *Fig. A20 – left panel*. It is the deepest transit in our sample (0.0135) and has a typical U-shape. We did not detect significant differences between the odd and even transits in this system, nor significant pre-transit brightening and post-transit brightening, nor significant variability in transit depth. This expected due to the long period nature of the candidate. Subsequently, we fitted the light curve with a model light curve (Fig. A20 – see left panel) and obtained transit residuals of this exoplanet candidate (Fig. A20 – mid panel). The residuals show that this transit can be reproduced well with the planetary model. We obtained quadratic limb darkening coefficients of $q_1 = 0.33(8)$ and $q_2 = 0.4(1)$. The best fit system parameters are: mid transit time $T_c = 454.9191(1)$, period $P = 15.35877$ days, planet-to-star radius ratio $R_p/R_s = 0.118(1)$, normalised semi-major axis $(R_p+R_s)/a = 0.038(1)$, and line-of-sight inclination $i = 89.1(1)$ (deg). The parameter $R_p/R_s = 0.01292$, presented by *Batalha et al. (2013)*, is very different from what we got for R_p/R_s, because it is a different candidate at a different period.

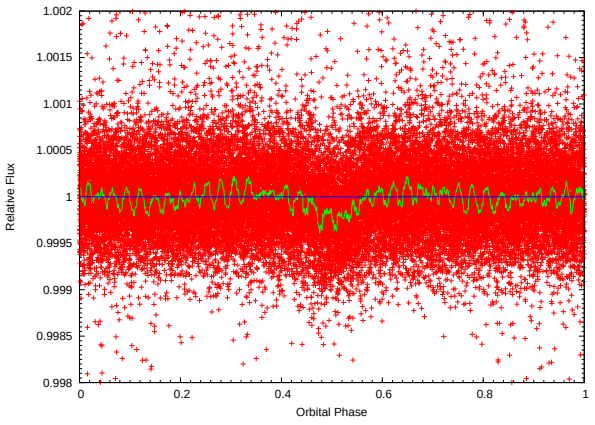

Fig. 15 The light curve of KIC5972334 phased to the orbital period $P = 0.7085982$ days, reported in *Batalha et al. (2013)*.

Finaly we searched for possible long-term changes of the orbital period. *Fig. A20 – right panel* shows that there is an indication for the long-term period change, with $\beta = 33.3316 \pm 11.9749$ d/Myr, which means that the period is potentially increasing. Since the PDM analysis indicated a potential period variation, we broke the light curve into segments of 2000 points in this case, and re-performed the T_c-free MCMC analysis. However, this analysis did not find any TTV signal.

5.9 Other exoplanet candidates

The candidates KIC6934291, KIC4055304, KIC10024051, KIC8235924, KIC10975146, KIC10028535, KIC10468885, KIC11600889, KIC8278371, KIC5513012, KIC10319385 and KIC9473078 did not show any peculiarities in their transit light curves, nor residuals (Fig. A6, A7, A8, A9, A11, A12, A13, A14, A15, A16, A17 and A19 – left and mid panels). These transits have typically shallow U-shapes. We did not detect significant differences between the odd and even transits in these systems. We fitted the light curves of these candidates with a theoretical light curve. The best fit parameters of all candidates are summarized in *Table 2*. We also improved the orbital periods reported in *Batalha et al. (2013)* via PDM and FA methods. Finaly we searched for possible long-term changes of the orbital periods. They are all listed in *Table 3*. *Fig. A6, A7, A8, A9, A11, A12, A13, A14, A15, A16, A17 and A19 – right panels* show that there are no significant evidences for the long-term period changes. In case of the exoplanet candidate KIC10468885 we detected an indication for the long-term period change with $\beta = 3.0$ d/Myr, which means that the period is increasing (Fig. A13 – right panel), however, based on the PDM Monte Carlo test, we could not consider this result as significant enough ($std = \pm 8.7$ d/Myr).

6 Summary and conclusions

Our main aim was to search for comet-like tails similar to KIC012557548b and for long-term orbital period variations. We were curious about frequency of comet-like tail formation among short-period Kepler exoplanet candidates. Close-in exoplanets, like KIC012557548b, are subjected to the greatest planet-star interactions. We therefore concentrated on the short-period exoplanet candidates with periods similar to KIC012557548b. We chose 20 exoplanet candidates observed by the Kepler mission, with the shortest orbital periods, ranging from 0.370 up to 0.708 days. We first improved the preliminary orbital periods (Batalha et al. 2013) and obtained the transit light curves of our exoplanet candidates. Subsequently, we searched for the signatures of a circum-planetary material in these light curves. For this purpose the final transit light curve of each planet was fitted with a theoretical light curve, and the residuals were examined for abnormalities. We also searched for possible long-term changes of the orbital period using the method of phase dispersion minimization (PDM). For candidates where the PDM analysis indicated potential period variations, we broke the light curve into segments of 2000/4000 points, and re-performed the T_c-free MCMC analysis. To test the effectiveness of our techniques, we first applied this procedure to KIC012557548b. The light curve of this

© 2006 WILEY-VCH Verlag GmbH & Co. KGaA, Weinheim

Table 2 An overview of the best fit parameters. Table contains the best fit qadratic limb darkening coefficients of the host stars (q_1 and q_2), and the best fit system parameters: mid transit time T_c, period P, planet-to-star radius ratio R_p/R_s, normalised semi-major axis $(R_p + R_s)/a$, and line-of-sight inclination i.

KIC Number	q_1	q_2	T_c (BKJD)	P (days)	R_p/R_s	$(R_p + R_s)/a$	i (deg)
3848972	0.9(1)	0.9(3)	534.34045(5)	0.37053	0.18(8)	0.71(4)	49(6)
8561063	0.0001(8)	0.7(1)	488.7930(1)	0.45329	0.044(4)	0.2(1)	76(2)
6666233	0.26(4)	0.8(1)	546.2643(5)	0.51241	0.016(2)	0.27(1)	85(4)
6047498	0.94(5)	0.95(4)	534.1331(3)	0.51873	0.3(2)	0.76(5)	43(5)
9030447	0.47(2)	0.99(2)	534.478(1)	0.56677	0.0091(1)	1.000(8)	85(1)
6934291	0.1(1)	0.2(2)	523.6117(4)	0.56786	0.018(8)	0.3(1)	74(14)
4055304	0.0006(3)	0.2(2)	546.2270(3)	0.57104	0.015(9)	0.24(1)	85(5)
10024051	0.55(2)	0.03(3)	553.9052(3)	0.57737	0.0187(4)	0.25(1)	86(3)
8235924	0.02(2)	0.3(3)	459.5745(4)	0.58800	0.018(3)	0.70(1)	47(1)
11774303	0.118(9)	0.7(2)	457.3181(7)	0.61408	0.07(4)	0.8(1)	37(11)
10975146	0.4(1)	0.8(1)	496.9595(4)	0.63133	0.0184(7)	0.24(1)	87(3)
10028535	0.1(1)	0.2(2)	454.9020(7)	0.66309	0.017(1)	0.21(1)	86(3)
10468885	0.03(3)	0.5(5	545.814(1)	0.66407	0.015(1)	0.26(6)	79(10)
11600889	0.29(7)	0.96(3)	550.4423(4)	0.66931	0.011(1)	0.40(9)	74(12)
8278371	0.06(5)	0.88(9)	484.1484(8)	0.67737	0.0086(5)	0.42(9)	73(15)
5513012	0.28(4)	0.87(3)	364.5110(5)	0.67934	0.0146(9)	0.25(2)	84(5)
10319385	0.02(1)	0.7(1)	584.0281(2)	0.68921	0.014(1)	0.79(7)	40(1)
9761199	0.94(5)	0.96(1)	533.1669(1)	0.69202	0.22(9)	0.43(3)	68(2)
9473078	0.7(4)	0.3(3)	574.852(1)	0.69384	0.010(4)	0.83(5)	35(5)
5972334	0.33(8)	0.4(1)	454.9191(1)	15.35877	0.118(1)	0.038(1)	89.1(1)

exoplanet is peculiar, caused by a pre-transit brightening, post-transit brightening and strong variability in the transit depth. Subsequently, we fitted the observed light curve with the theoretical model light curve, assuming a spherical planet, and obtained transit residuals. We observed a significant fluctuation in these residuals. We then searched for a long-term orbital period variation using the PDM method. Previously, *Budaj (2013)* obtained $\beta = 0.3 \pm 0.5$ d/Myr using 14 quarters of Kepler data, indicating no change in the transit period. We repeated the analysis using 17 quarter of data, revealing no significant long-term period variation.

We then analyzed the transit light curves and residuals of our sample similarly as per KIC012557548b. We searched for significant fluctuations in these residuals, strong variabilities in the transit depth, pre-transit and post-transit brightenings in light curves, which could indicate presence of the circum-planetary material. In 8 cases out of 20 we found some interesting peculiarities (KIC3848972, KIC8561063, KIC6666233, KIC6047498, KIC9030447, KIC11774303, KIC9761199, KIC5972334). We found 4 cases of exoplanet candidates with relatively deep V-shape of the transits (KIC3848972, KIC8561063, KIC6047498, KIC9761199). We detected differences between the odd and even transits in 5 cases (KIC3848972, KIC6666233, KIC6047498, KIC11774303, KIC9761199). In cases of KIC3848972, KIC8561063, KIC6666233, KIC6047498, KIC11774303 and KIC9761199 we consider the eclipsing binary alternative as possible. Excepting KIC11774303, the PDM/FA based two times alias orbital period is also possible. We found 2 cases of exoplanet candidates with sinusoidal out-of-transit periodic background variability, which is very similar to an RS Canum Venaticorum-like distortion wave (KIC3848972 and KIC9761199). In addition, the sinusoidal background variability shifted in phase during the Kepler observations, suggesting that it is not due to Doppler beaming. The background variations may potentially be due to stellar spot modulation. The exoplanet candidate KIC9030447 is also peculiar, because its light curve shows a small brightening, approximately half a phase from the transit, and a secondary eclipse-like signal approximately at phase 0.85. Further we discovered that these additional features of the light curve slighly shifted in phase during the Kepler observations. Moreover, the secondary eclipse-like signal is changing its depth. That is why we consider the eclipsing binary on eccentric orbit alternative as more possible as exoplanet transits or stellar pulsations.

None of the exoplanet candidates shows signs of a comet-like tail. We did not find any significant fluctuations in residuals, strong variabilities in the transit depth, nor pre-transit and post-transit brightenings in light curves. We found only a linear downward/upward residual trend from sine-like background variability in cases of exoplanet candidates KIC3848972 and KIC9761199, and a small residual fluctuation in case of exoplanet candidate KIC9030447 due to the poor fit. It seems that the frequency of comet-like tail formation among short-period Kepler exoplanet candidates is very low. We searched for comet-like tails based on the period criterion. Based on our results we can conclude that the short-period criterion is not enough to cause comet-like tail formation. This result is in agreement with the theory of

© 2006 WILEY-VCH Verlag GmbH & Co. KGaA, Weinheim

Table 3 An overview of improved orbital periods. Exoplanet candidates signed at their KIC Number with $*$ may have twice as long orbital period. We did not confirm the preliminary orbital period in case of candidate KIC5972334. Table also contains the β parameter.

KIC Number	Period by *Batalha et al. (2013)* (days)	Period by PDM (days)	Period by FA (days)	Period by MCMC (days)	β (d/Myr)
3848972*	0.3705290	0.37052870	0.37052750	0.37053	-0.8 $\pm$ 1.4
8561063*	0.4532875	0.45328705	0.45328830	0.45329	0.92 $\pm$ 0.93
6666233*	0.5124040	0.51240883	0.51240860	0.51241	-1.0 $\pm$ 2.3
6047498*	0.5187486	0.51872845	0.51872930	0.51873	-15.0 $\pm$ 1.9
9030447	0.5667281	0.56670873	0.56680630	0.56677	0.9 $\pm$ 8.6
6934291	0.5678562	0.56785838	0.56785920	0.56786	-1.0 $\pm$ 4.0
4055304	0.5710391	0.57103788	0.57104400	0.57104	1.0 $\pm$ 49.7
10024051	0.5773752	0.57737694	0.57736750	0.57737	0.9 $\pm$ 1.6
8235924	0.5879933	0.58800171	0.58800290	0.58800	1.0 $\pm$ 1.8
11774303	0.6140747	0.61408403	0.61409220	0.61408	0.9 $\pm$ 2.9
10975146	0.6313298	0.63133287	0.63133840	0.63133	-1.0 $\pm$ 1.4
10028535	0.6630983	0.66308772	0.66307940	0.66309	-1.0 $\pm$ 3.6
10468885	0.6640818	0.66407462	0.66406930	0.66407	3.0 $\pm$ 8.7
11600889	0.6693163	0.66931924	0.66930920	0.66931	1.0 $\pm$ 1.2
8278371	0.6773911	0.67737580	0.67737370	0.67737	-1.0 $\pm$ 3.3
5513012	0.6793614	0.67933835	0.67933710	0.67934	0.9 $\pm$ 3.1
10319385	0.6892040	0.68920953	0.68920870	0.68921	-1.0 $\pm$ 10.9
9761199*	0.6920069	0.69201741	0.69204530	0.69202	-3.0 $\pm$ 0.4
9473078	0.6938521	0.69384010	0.69383390	0.69384	1.0 $\pm$ 7.3
5972334	0.7085982	15.35747382	15.36051120	15.35877	33.3 $\pm$ 11.9

the thermal wind and planet evaporation (Perez-Becker & Chiang 2013). This theory predicts that catastrophic evaporation, which leads into creation of a comet-like tail, can occure only in relatively low-mass planets with masses less than that of Mercury. Since all the exoplanet candidates out of 20 have planet-to-star radius ratio higher than 0.003 (see parameter R_p/R_s in Table 2; the value 0.003 approximately valids for the planet Mercury), they are likely to be more massive than Mercury and, consequently, lack the catastrophic evaporation contrary to KIC012557548b.

We also found 3 cases of candidates (KIC6047498, KIC9761199 and KIC5972334) which showed some changes of the orbital period. In one case (KIC5972334) we observed an orbital period increasing, other exoplanet candidates showed orbital period shortenings. Since the PDM analysis indicated a potential period variation in these cases, we broke the light curve into segments of 2000/4000 points, and re-performed the T_c-free MCMC analysis. In case of exoplanet candidate KIC6047498 we found a semi-periodic TTV signal associated with the transit, indicative of an outer companion with an orbital period of $>$ 2000 days. In case of exoplanet candidate KIC9761199 this analysis also confirmed our results from the PDM analysis about long-term period change and revealed a periodic TTV signal with a period of $\sim$ 1500 days, indicative of a possible massive outer companion. In case of exoplanet candidate KIC5972334 this analysis did not find any TTV signal. Based on our results we can see that orbital period changes are not caused by comet-like tail disintegration processes, but rather by possible massive outer companions. Moreover, nor KIC012557548b with comet-like tail disintegration, did not show any long-term orbital period variation.

We also improved the preliminary orbital periods using PDM/FA methods. We did not confirm the preliminary orbital period in case of exoplanet candidate KIC5972334. We obtained period $P = 15.35747382$ days using the PDM and $P = 15.36051120$ days using the FA method, which is in the agreement with period $P = 15.359$ days found by *Steffen et al. (2010)*. We did not confirm the second transiting object with *P* over 2.420 days in this system, suggested by the same authors. The exoplanet candidates KIC3848972, KIC8561063, KIC6666233, KIC6047498 and KIC9761199 may have twice as long orbital period.

Acknowledgements. The authors thank Dr. L. Hambálek and Dr. T. Krejčová for the technical assistance, comments and discussions. This work was supported by the VEGA grants of the Slovak Academy of Sciences Nos. 2/0143/14, 2/0038/13, by the Slovak Research and Development Agency under the contract No. APVV-0158-11, and by the realization of the Project ITMS No. 26220120029, based on the Supporting Operational Research and Development Program financed from the European Regional Development Fund. JB was supported by the Australian Research Council through DP120101792. GZ thanks Chelsea X. Huang for her contribution to the light curve fitting program.

© 2006 WILEY-VCH Verlag GmbH & Co. KGaA, Weinheim

References

Agol, E., Steffen, J., Sari, R. & Clarkson, W.: 2005, MNRAS 359, 567
Batalha, N.M., Rowe, J.F., Bryson, S.T., et al.: 2013, ApJS 204, 24
Bodenheimer, P., Lin, D.N.C. & Mardling, R.A.: 2001, ApJ 548, 466
Borucki, W.J., Koch, D.G., Basri, G., et al.: 2011, ApJ 736, 19
Borucki, W.J., Koch, D.G., Batalha, N., et al.: 2012, ApJ 745, 120
Bourrier, V., Lecavelier des Etangs, A., Dupuy, H., et al.: 2013, A&A 551, 63
Brogi, M., Keller, C.U., de Juan Ovelar, M., Kenworthy, M.A., de Kok, R.J., Min, M. & Snellen, I.A.G.: 2012, A&A 545, 5
Budaj, J.: 2013, A&A 557, 72
Burrows, A., Budaj, J. & Hubeny, I.: 2008, ApJ 678, 1436
Burrows, A. & Lunine, J.: 1995, Natur 378, 333
Colón, K.D., Ford, E.B. & Morehead, R.C.: 2012, MNRAS 426, 342
Croll, B., Rappaport, S., DeVore, J., et al.: 2014, ApJ 786, 100
Esteves, L.J. De Mooij, E.J.W. & Jayawardhana, R.: 2013, ApJ 772, 51
Faigler, S. & Mazeh, T.: 2011, MNRAS 415, 3921
Ford, E.B., Fabrycky, D.C., Steffen, J.H., et al.: 2012, ApJ 750, 113
Ford, E.B., Rowe, J.F., Fabrycky, D.C., et al.: 2011, ApJ 197, 2
Foreman-Mackey, D., Hogg, D.W., Lang, D., & Goodman, J.: 2013, PASP 125, 306
Fortney, J.J., Lodders, K., Marley, M.S. & Freedman, R.S.: 2008, ApJ 678, 1419
Fressin, F., Torres, G., Rowe, J.F., et al.: 2012, Natur 482, 195
Guillot, T., Burrows, A., Hubbard, W.B., Lunine, J.I. & Saumon, D.: 1996, ApJ 459, 35
Holman, M.J. & Murray, N.W.: 2005, Sci 307, 1288
Hubbard, W.B., Hattori, M.F., Burrows, A., Hubeny, I. & Sudarsky, D.: 2007, Icar 187, 358
Hubeny, I., Burrows, A. & Sudarsky, D.: 2003, ApJ 594, 1011
Jackson, B., Stark, C.C., Adams, E.R., Chambers, J. & Deming, D.: 2014, AAS 223, 202
Kawahara, H., Hirano, T., Kurosaki, K., Ito, Y. & Ikoma, M.: 2013, ApJ 776, L6
Kipping, D.M.: 2013, MNRAS 435, 2152
Knutson, H.A., Charbonneau, D., Allen, L.E., Burrows, A. & Megeath, S.T.: 2008, ApJ 673, 526
Kulow, J.R., France, K., Linsky, J. & Loyd, R.O.P.: 2014, ApJ 786, 132
Kurokawa, H. & Kaltenegger, L.: 2013, MNRAS 433, 3239
Lecavelier des Etangs, A., Ehrenreich, D., Vidal-Madjar, A. et al.: 2010, A&A 514, 72
Loeb, A. & Gaudi, B.S.: 2003, ApJ 588, 117
Lopez, E.D., Fortney, J.J. & Miller, N.: 2012, ApJ 761, 59
Luddington, E.W.: 1978, BAAS 10, 418
Maciejewski, G., Dimitrov, D., Seeliger, M., et al.: 2013, A&A 551, 108
Mandel, K. & Agol, E.: 2002, ApJ 580, 171
Mazeh, T., Nachmani, G., Holczer, T., et al.: 2013, ApJS 208, 16
Ofir, A. & Dreizler, S.: 2013, A&A 555, 580
Owen, J.E. & Wu, Y.: 2013, ApJ 775, 1050
Rappaport, S., Barclay, T., DeVore, J., Rowe, J., Sanchis-Ojeda, R., Still, M.: 2014, ApJ 784, 40
Rappaport, S., Levine, A., Chiang, E., et al.: 2012, ApJ 752, 1
Rybicki, G.B. & Lightman, A.P.: 1979, Radiative Processes in Astrophysics, Wiley, New York
Perez-Becker, D. & Chiang, E.: 2013, MNRAS 433, 2294
Sanchis-Ojeda, R., Rappaport, S., Winn, J.N., Kotson, M.C., Levine, A.M., El Mellah, I.: 2014, ApJ 787, 47
Slawson, R.W., Prša, A., Welsh, W.F., et al.: 2011, AJ 142, 160
Steffen, J.H., Batalha, N.M., Borucki, W.J., et al.: 2010, ApJ 725, 1226
Steffen, J.H., Ford, E.B., Rowe, J.F., et al.: 2012, ApJ 756, 186
Stellingwerf, R.F.: 1978, ApJ 224, 953
Stellingwerf, R.F.: 2004, PDM2, Stellingwerf Consulting, Huntsville 2004
Tassoul, J.L. & Tassoul, M.: 1992, ApJ 395, 259
Tian, F., Toon, O.B., Pavlov, A.A. & De Sterck, H.: 2005, ApJ 621, 1049
van Werkhoven, T.I.M., Brogi, M., Snellen, I.A.G. & Keller, C.U.: 2014, A&A 561, A3
Vidal-Madjar, A., Désert, J.-M., Lecavelier des Etangs, A., et al.: 2004, ApJ 604, 69
Vidal-Madjar, A., Lecavelier des Etangs, A., Désert, J.-M., Ballester, G.E., Ferlet, R., Hébrard, G. & Mayor, M.: 2003, Natur 422, 143
Yelle, R.V.: 2004, Icar 170, 167
Zahn, J.P.: 1977, A&A 57, 383

© 2006 WILEY-VCH Verlag GmbH & Co. KGaA, Weinheim

A An overview of light curves, transit residuals, and long-term changes of the orbital periods

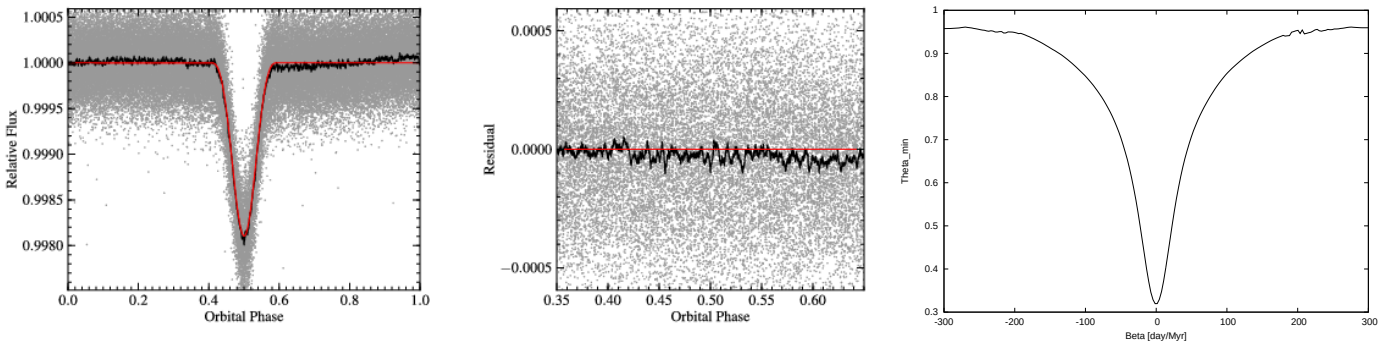

Fig. A1 The light curve (left panel), transit residuals (mid panel), and the long-term change of orbital period (right panel) of the exoplanet candidate KIC3848972.

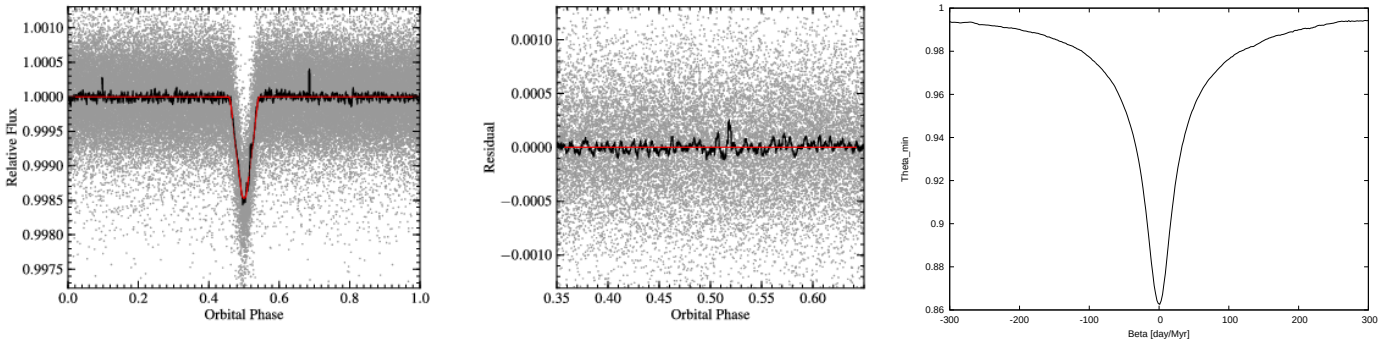

Fig. A2 The light curve (left panel), transit residuals (mid panel), and the long-term change of orbital period (right panel) of the exoplanet candidate KIC8561063.

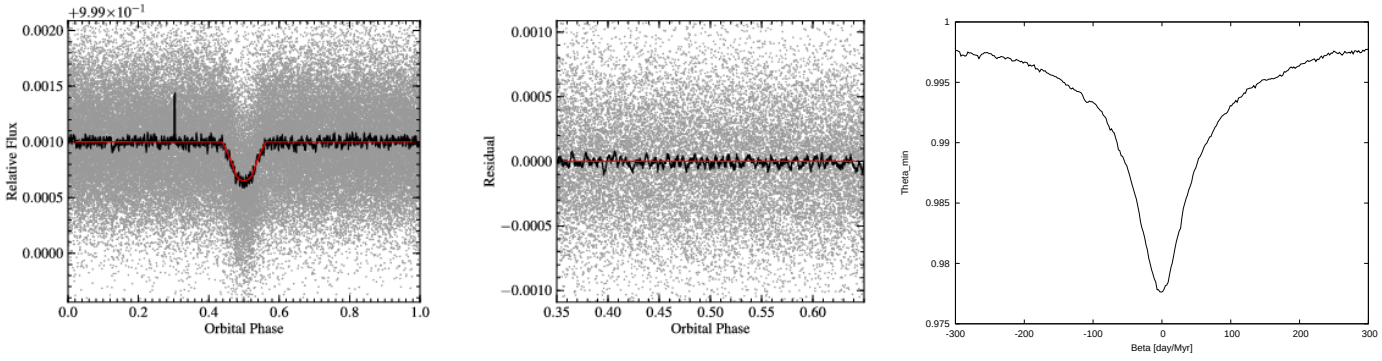

Fig. A3 The light curve (left panel), transit residuals (mid panel), and the long-term change of orbital period (right panel) of the exoplanet candidate KIC6666233.

© 2006 WILEY-VCH Verlag GmbH & Co. KGaA, Weinheim

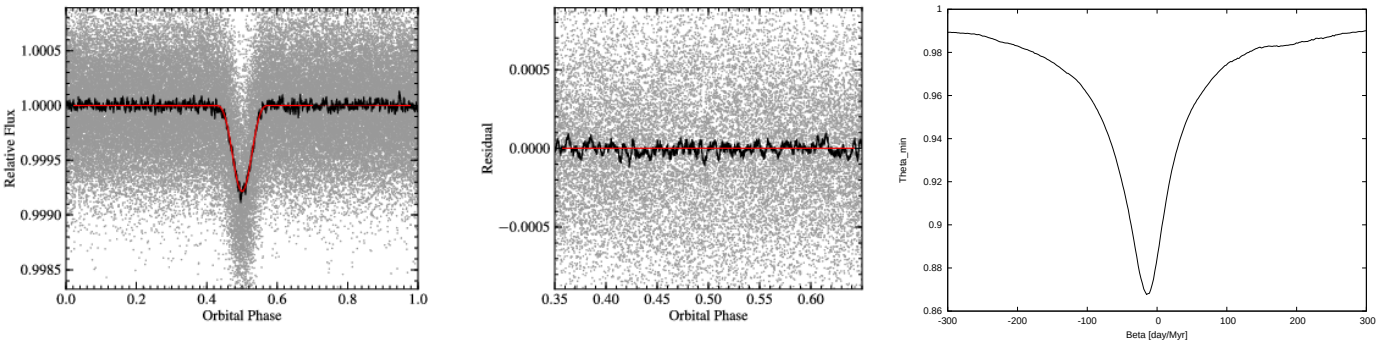

Fig. A4 The light curve (left panel), transit residuals (mid panel), and the long-term change of orbital period (right panel) of the exoplanet candidate KIC6047498.

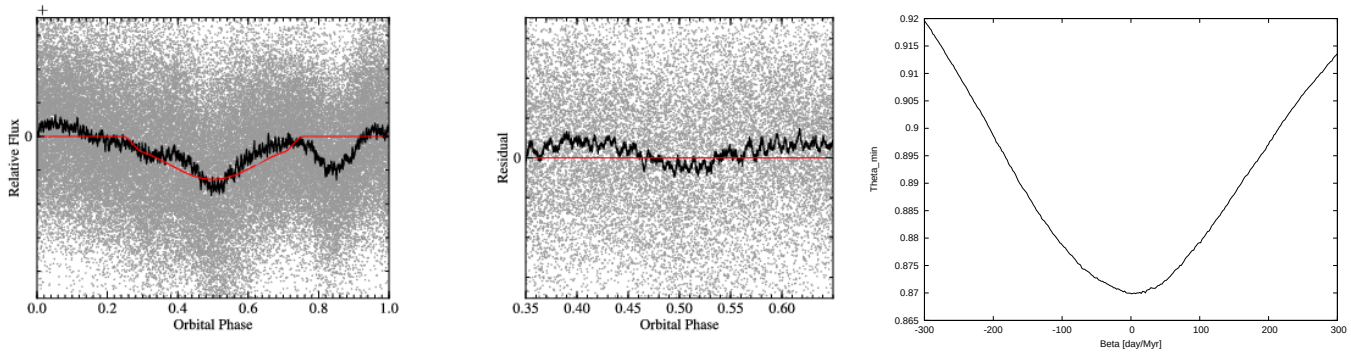

Fig. A5 The light curve (left panel), transit residuals (mid panel), and the long-term change of orbital period (right panel) of the exoplanet candidate KIC9030447.

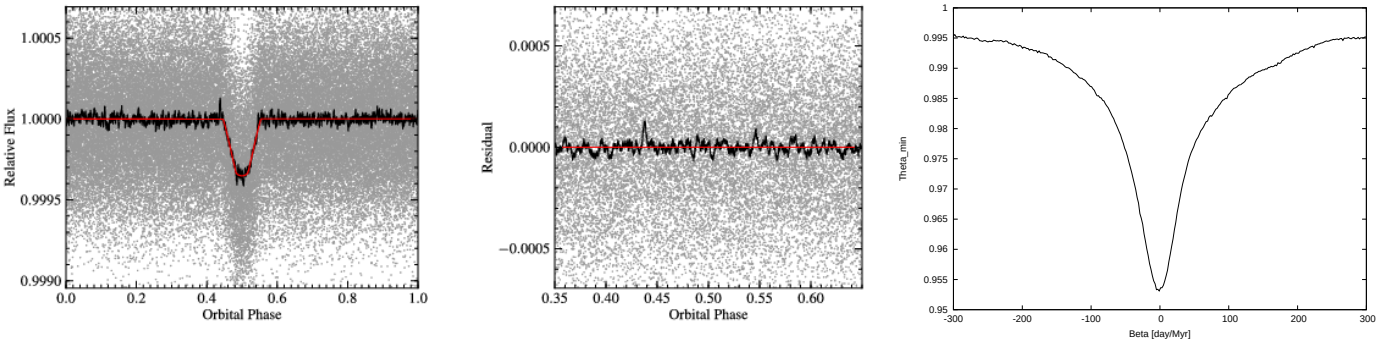

Fig. A6 The light curve (left panel), transit residuals (mid panel), and the long-term change of orbital period (right panel) of the exoplanet candidate KIC6934291.

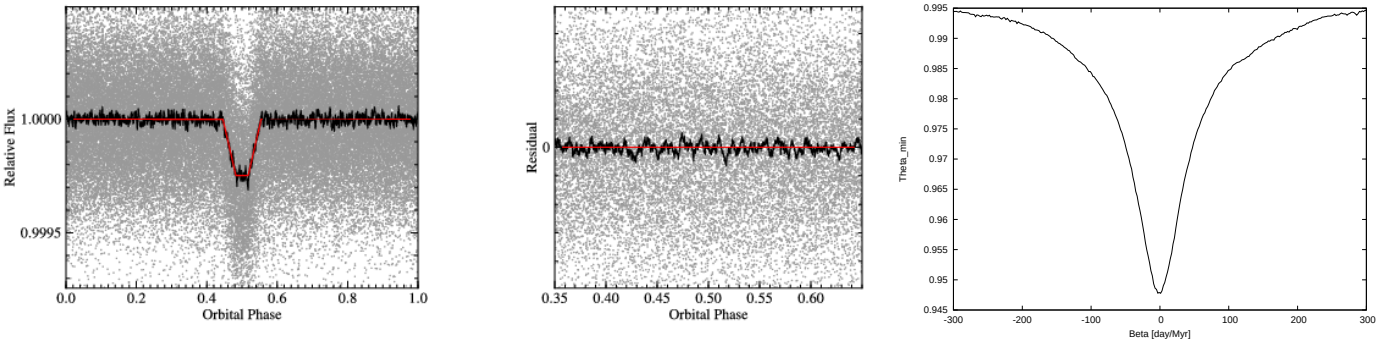

Fig. A7 The light curve (left panel), transit residuals (mid panel), and the long-term change of orbital period (right panel) of the exoplanet candidate KIC4055304.

© 2006 WILEY-VCH Verlag GmbH & Co. KGaA, Weinheim

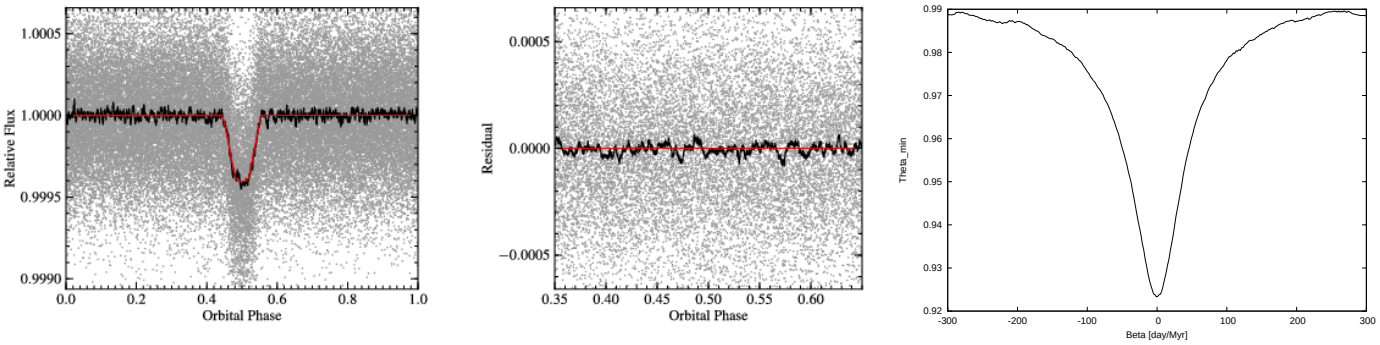

Fig. A8 The light curve (left panel), transit residuals (mid panel), and the long-term change of orbital period (right panel) of the exoplanet candidate KIC10024051.

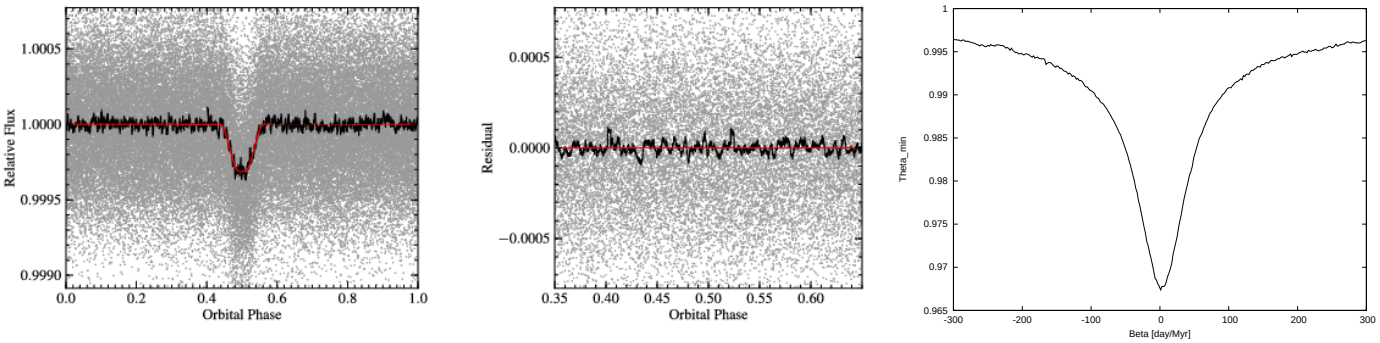

Fig. A9 The light curve (left panel), transit residuals (mid panel), and the long-term change of orbital period (right panel) of the exoplanet candidate KIC8235924.

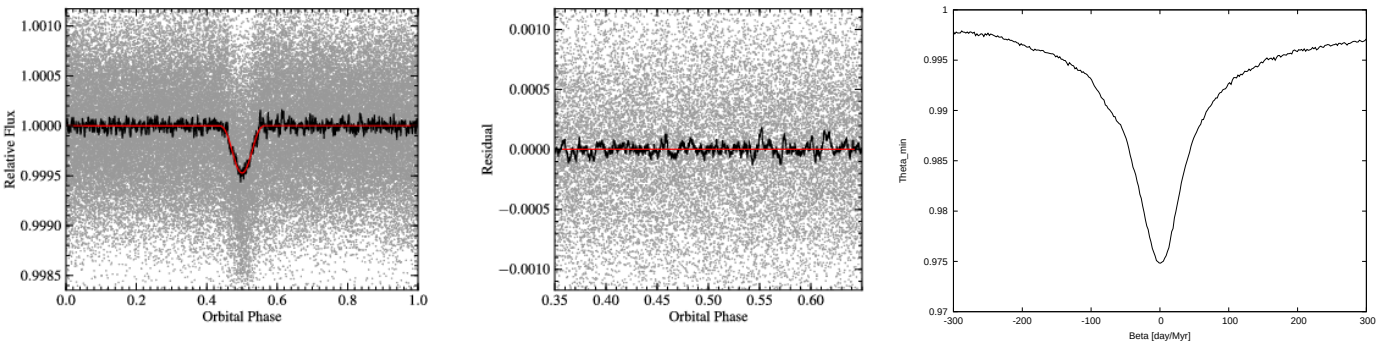

Fig. A10 The light curve (left panel), transit residuals (mid panel), and the long-term change of orbital period (right panel) of the exoplanet candidate KIC11774303.

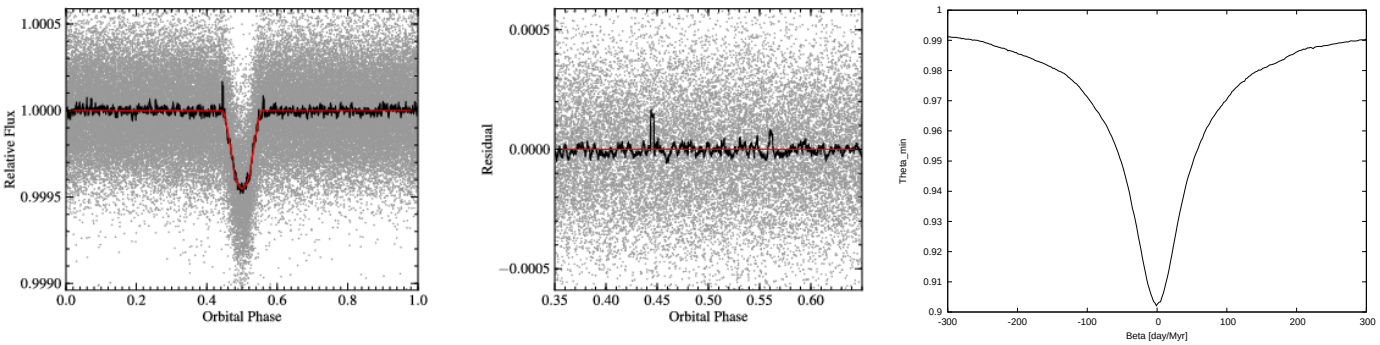

Fig. A11 The light curve (left panel), transit residuals (mid panel), and the long-term change of orbital period (right panel) of the exoplanet candidate KIC10975146.

© 2006 WILEY-VCH Verlag GmbH & Co. KGaA, Weinheim

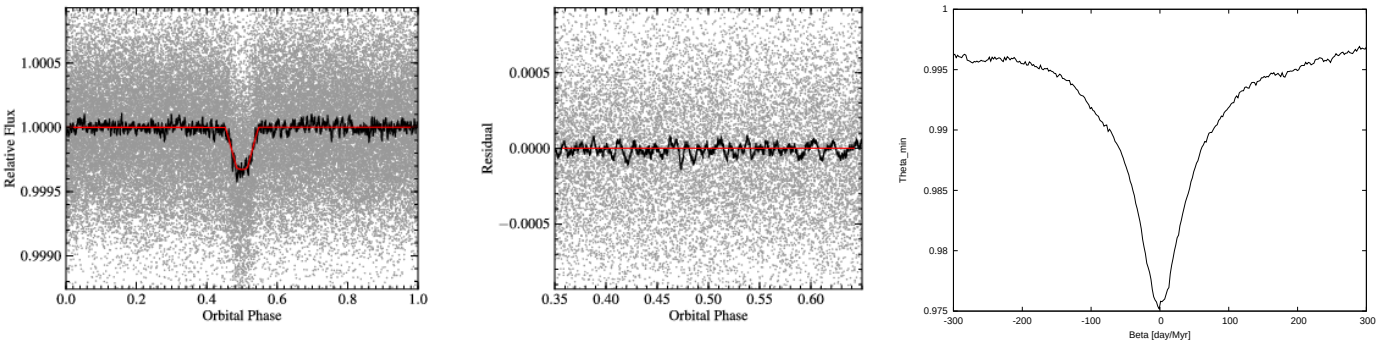

Fig. A12 The light curve (left panel), transit residuals (mid panel), and the long-term change of orbital period (right panel) of the exoplanet candidate KIC10028535.

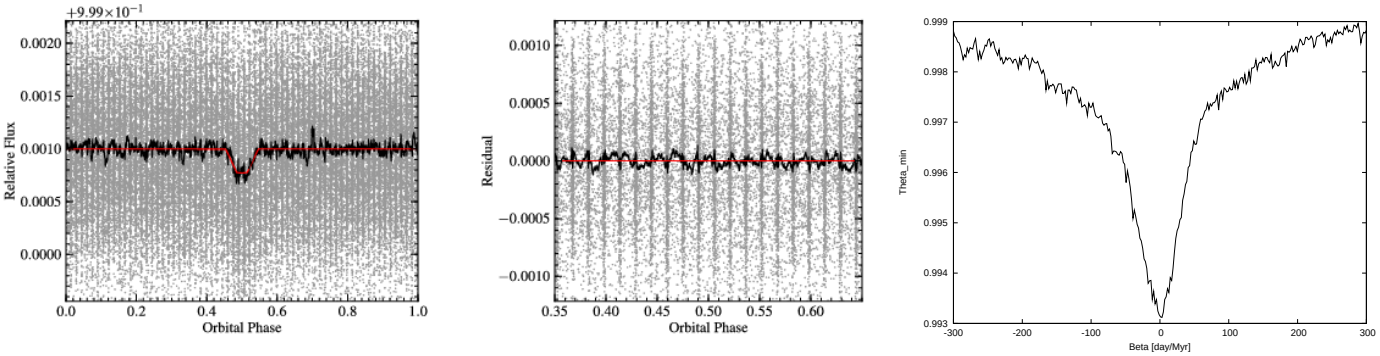

Fig. A13 The light curve (left panel), transit residuals (mid panel), and the long-term change of orbital period (right panel) of the exoplanet candidate KIC10468885.

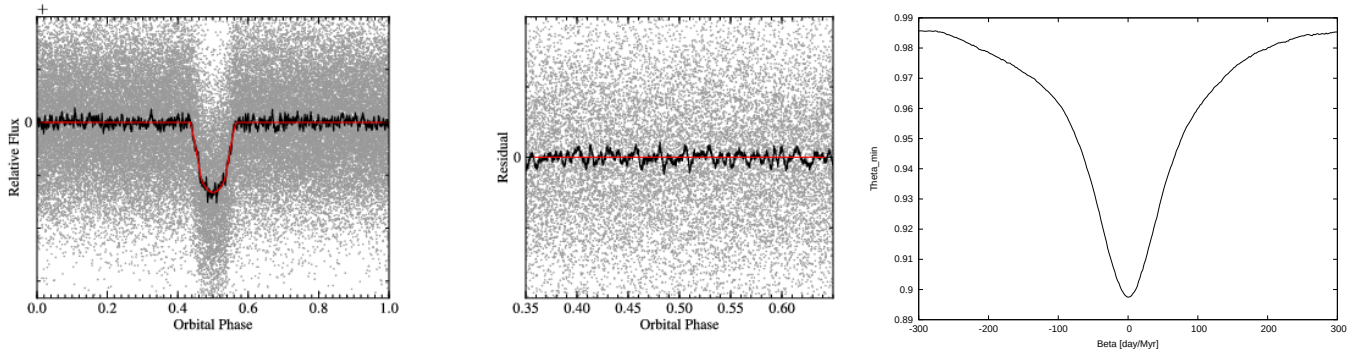

Fig. A14 The light curve (left panel), transit residuals (mid panel), and the long-term change of orbital period (right panel) of the exoplanet candidate KIC11600889.

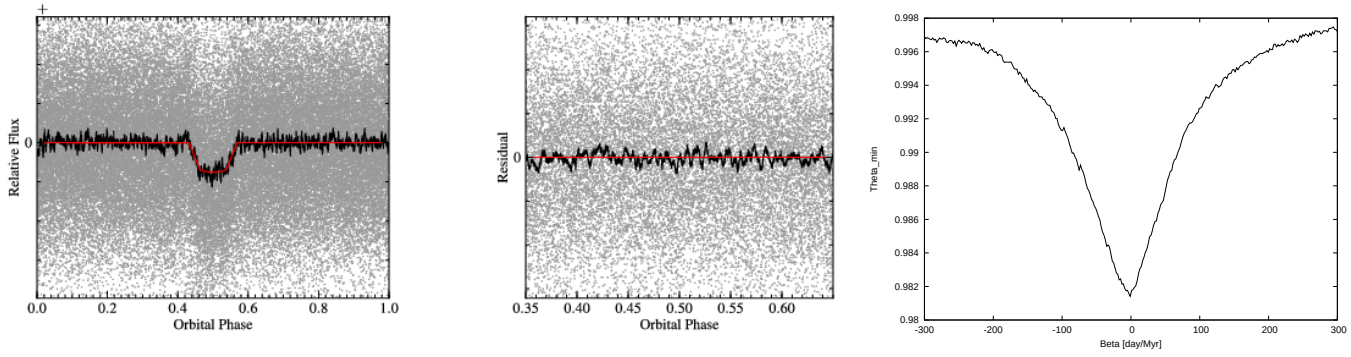

Fig. A15 The light curve (left panel), transit residuals (mid panel), and the long-term change of orbital period (right panel) of the exoplanet candidate KIC8278371.

© 2006 WILEY-VCH Verlag GmbH & Co. KGaA, Weinheim

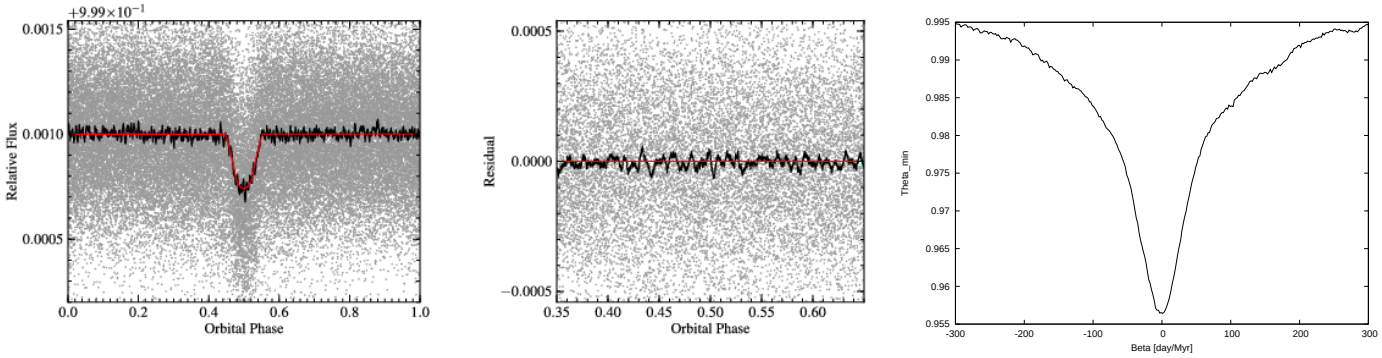

Fig. A16 The light curve (left panel), transit residuals (mid panel), and the long-term change of orbital period (right panel) of the exoplanet candidate KIC5513012.

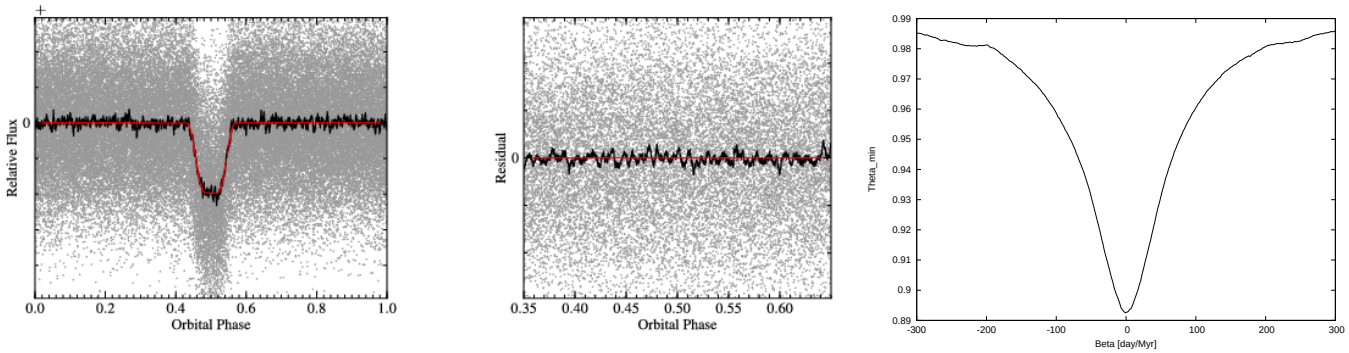

Fig. A17 The light curve (left panel), transit residuals (mid panel), and the long-term change of orbital period (right panel) of the exoplanet candidate KIC10319385.

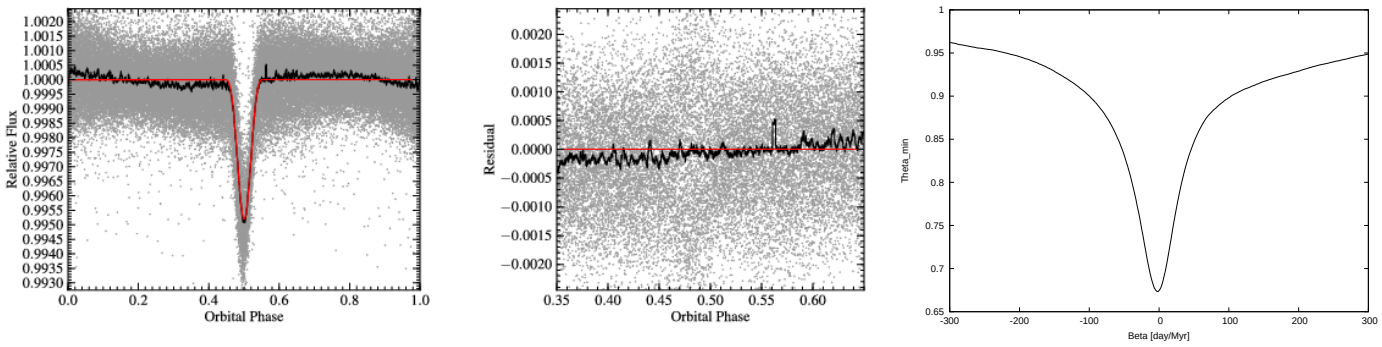

Fig. A18 The light curve (left panel), transit residuals (mid panel), and the long-term change of orbital period (right panel) of the exoplanet candidate KIC9761199.

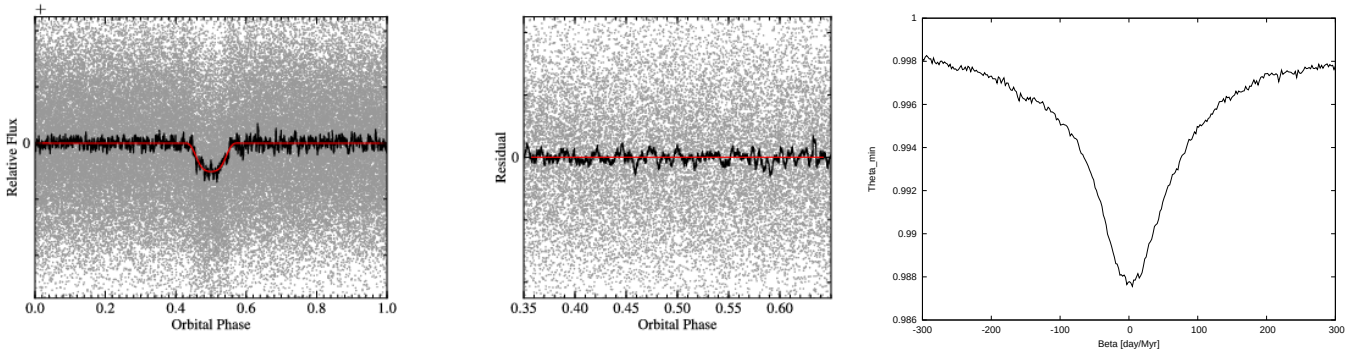

Fig. A19 The light curve (left panel), transit residuals (mid panel), and the long-term change of orbital period (right panel) of the exoplanet candidate KIC9473078.

© 2006 WILEY-VCH Verlag GmbH & Co. KGaA, Weinheim

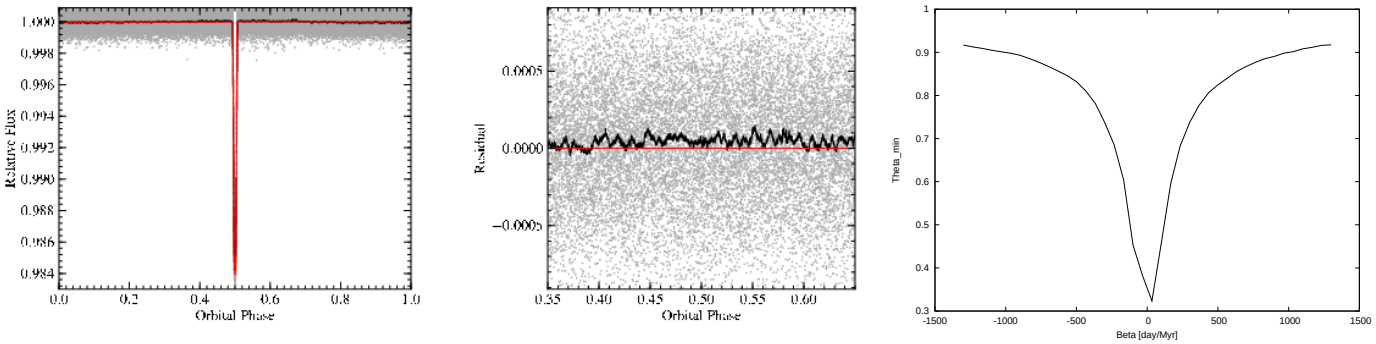

Fig. A20 The light curve (left panel), transit residuals (mid panel), and the long-term change of orbital period (right panel) of the exoplanet candidate KIC5972334.

© 2006 WILEY-VCH Verlag GmbH & Co. KGaA, Weinheim